International Journal of Pharmaceutics 431 (2012) 210–221

Contents lists available at SciVerse ScienceDirect

International Journal of Pharmaceutics

journal homepage: www.elsevier.com/locate/ijpharm

Pharmaceutical Nanotechnology

Calcium phosphate embedded PLGA nanoparticles: A promising gene delivery vector with high gene loading and transfection efficiency

Jie Tang[a,b], Jin-Ying Chen[a], Jing Liu[a], Min Luo[a], Ying-Jing Wang[a], Xia-wei Wei[b], Xiang Gao[a], Bi-lan Wang[a], Yi-Bo Liu[a], Tao Yi[a,c], Ai-Ping Tong[a], Xiang-Rong Song[a], Yong-Mei Xie[a], Yinglan Zhao[a], Mingli Xiang[a], Yuan Huang[b], Yu Zheng[a,*]

[a] College of Pharmacy, State Key Laboratory of Biotherapy, Sichuan University, No. 17, Section 3, Renmin Nan Road, Chengdu 610041, PR China
[b] West China School of Pharmacy, Sichuan University, No. 17, Section 3, Renmin Nan Road, Chengdu, Sichuan 610041, PR China
[c] Department of Gynecology and Obstetrics, Key Laboratory of Obstetric and Gynecologic and Pediatric Diseases and Birth Defects of Ministry of Education, West China Second Hospital, PR China

ARTICLE INFO

Article history:
Received 9 December 2011
Received in revised form 27 March 2012
Accepted 17 April 2012
Available online 23 April 2012

Keywords:
CaPi-pDNA-PLGA-NPs
PLGA nanoparticle
Calcium phosphate
Plasmid DNA
HEK293

ABSTRACT

In the purpose of increasing incorporation efficiency and improving the release kinetics of plasmid DNA (pDNA) from poly(D,L-lactide-co-glycolide) (PLGA) nanoparticles, a facile method for the fabrication of calcium phosphate (CaPi) embedded PLGA nanoparticles (CaPi-pDNA-PLGA-NPs) was developed. The effect of several preparation factors on the particle size, incorporation efficiency, pDNA release and transfection efficiency in vitro was studied by Single Factor Screening Method. These preparation factors included the molecular weight (MW), hydrolysis degree (HD) of polyvinyl alcohol (PVA), sonication power and time, composition of organic phase, initial concentration of calcium phosphate and calcium (Ca) to phosphate ion (P) ratio (Ca/P ratio), etc. The CaPi-pDNA-PLGA-NPs made according to the optimal formulation were spherical in shape observed by transmission electron microscopy (TEM) with a mean particle size of 207 ± 5 nm and an entrapment efficiency of $95.7 \pm 0.8\%$. Differential scanning calorimetry (DSC) suggested that there existed interaction between the DNA-calcium-phosphate (CaPi-pDNA) complexes and the polymeric matrices of PLGA. X-ray diffractometry (XRD) further proved the conclusion and indicated that the CaPi-pDNA was in weak crystallization form inside the nanoparticles. The Brunauer–Emmett–Teller (BET) surface area measurement demonstrated that the CaPi-pDNA-PLGA-NPs are mesoporous with specific surface area of 57.5 m^2/g and an average pore size of 96.5 Å. The transfection efficiency of the CaPi-pDNA-PLGA-NPs on human embryonic kidney 293 (HEK 293) cells in vitro was $22.4 \pm 1.2\%$, which was much higher than those of both the pDNA loaded PLGA nanoparticles (pDNA-PLGA-NPs) and the CaPi-pDNA embedded PLGA microparticles (CaPi-pDNA-PLGA-MPs). The CaPi-pDNA-PLGA-NPs are promising vectors for gene delivery.

1. Introduction

Effective gene delivery is an imperative goal for many research groups because gene therapy is becoming a promising approach for the treatment of disease (Ochiya et al., 2001). DNA is a negatively charged macromolecule, which hinders its entry into the tumor cells through the negatively charged lipid bilayer. For this reason, DNA needs to be condensed and have its charge neutralized before entry (Ledley, 1996). Due to the defects of viral delivery system including limits on the size of the plasmid, lack of tissue specificity, lack of safety (Navarro et al., 1998), it has been used only for ex vivo gene therapy (Van de Wetering et al., 1998; Tagawa et al., 2002). Non-viral gene delivery systems are gaining recognition as an alternative to viral gene vectors for their potential in avoiding the problems associated with the viral systems (Luten et al., 2007). Therefore, non-viral delivery systems made of biodegradable polymers have been widely explored as carriers for pDNA over the last decade (Gao et al., 2007).

PLGA is composed of lactic and glycolic acids linked together by ester bonds. The polymer degradation proceeds with formation of free carboxylic end groups (Labhasetwar et al., 1999). Incorporation of pDNA into PLGA particles provides (1) preservation of pDNA from in vivo degradation, (2) controlled release of the pDNA, and (3) a transfection vector for mammalian cells (Blum and Saltzman, 2008). PLGA based delivery system for pDNA has been widely studied and demonstrated effective (Hedley, 2003; Walter et al., 2001; Wang et al., 1999; Denis-Mize et al., 2003; He et al., 2005a,b; Lima et al., 2003; Coelho et al., 2006).

* Corresponding author. Tel.: +86 28 85503817; fax: +86 28 85164060.
E-mail address: zhengyu_iris@163.com (Y. Zheng).

0378-5173/$ – see front matter © 2012 Elsevier B.V. All rights reserved.
http://dx.doi.org/10.1016/j.ijpharm.2012.04.046

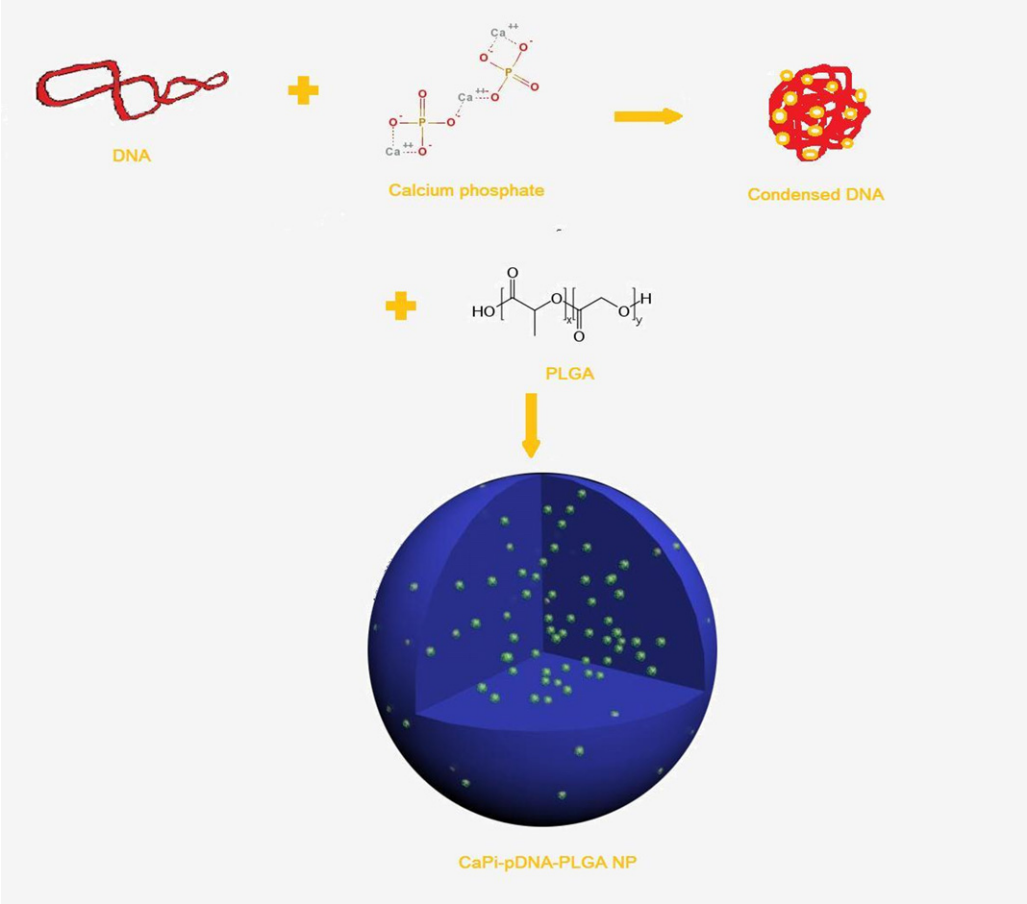

Fig. 1. Preparation scheme of CaPi-pDNA-PLGA-NPs.

Generally speaking, the rate of pDNA release from conventional PLGA based delivery system is too slow (Walter et al., 1999; Zhu et al., 2000) to induce immune responses as (1) the cumulative release of pDNA was too small to induce effects, (2) changes in the structure of pDNA was induced in the acidic microenvironment developed within the interior of the PLGA particles. Another limitation of PLGA based delivery vehicle is the low encapsulation efficiency of hydrophilic molecules such as pDNA. This inherent problem is further compounded when submicron particles are fabricated (Blum and Saltzman, 2008). Recently, a new delivery system that incorporates CaPi-DNA co-precipitate into PLGA microparticles was explored (Li et al., 2004). Since CaPi-pDNA co-precipitate has excellent biocompatibility, biodegradability and adsorptive capacity for pDNA, the CaPi-pDNA PLGA micron delivery system has demonstrated a better pDNA loading efficiency and better protection of pDNA relative to PLGA based micron delivery system itself (Li et al., 2004). Unfortunately, there are some obvious drawbacks of this PLGA micron system such as slow release of pDNA and consequently low transfection efficiency in vitro due to the large size of the carrier (Aral and Akbuga, 2003; Wang et al., 1999; Tinsley-Bown et al., 2000). Orrantia and Chang (1990), by tracing ^{32}P-marked DNA inside the cell, concluded that the particle size of nanoscale helped the protection of pDNA from degrading enzymes. Loyter et al. (1982) has also emphasized the importance of the nanoscaled particle size after studying the intracellular transport of ^{3}H-marked DNA. And in some cell lines, only the submicron size particles are taken up efficiently other than microparticles (e.g. Hepa 1–6, HepG2, and KLN 205) (Zauner et al., 2001). These studies revealed the importance of the particle size in gene transfection efficiency.

Here we report a simple and reproducible method to prepare well-defined CaPi-pDNA PLGA nanoparticles for the incorporation of pDNA, which will (1) enhance pDNA encapsulation within the particle, (2) provide an ideal release rate of pDNA, and (3) increase transfection efficiency in vitro. The preparation scheme of CaPi-pDNA-PLGA-NPs is presented in Fig. 1. CaPi-pDNA complexes were added to the aqueous phase when preparing the nanoparticles. After the evaporation of the solvent in organic phase, the complexes were embedded in the PLGA matrices.

2. Materials and methods

2.1. Materials

PLGA including PLGA 50:50 (lactide:glycoside, MW = 15 kDa), PLGA 50:50 (MW = 40–75 kDa), PVA with different degrees of hydrolyzation and polymerization (MW: 9000–10,000, HD: 80%; MW: 13,000–23,000, HD: 87%; MW: 30,000–50,000, HD: 87%; MW: 30,000–70,000, HD: 90%) and Hoechst 33258 reagent were purchased from Sigma–Aldrich. Plasmid DNA (pGFP) was extracted from cultured *Escherichia coli* with Qiagen's EndoFree Plasmid Giga Kit (Santa Clara, CA). Agarose gel (0.8%) electrophoretic analysis showed that the plasmid was mainly in supercoiled form. All other chemicals used were analytical grade reagent.

2.2. Formulation screening of CaPi-pDNA-PLGA-NPs

2.2.1. Preparation of CaPi-pDNA-PLGA-NPs

A phosphate precursor solution with various pH was comprised 0.28 M NaCl, 10 mM KCl, 50 mM dextrose, 40 mM HEPES and

various concentration of Na_2HPO_4. A calcium precursor solution was comprised pDNA and various concentration of $CaCl_2$ which was made 30 min before use.

CaPi-pDNA-PLGA-NPs were prepared by a water-in–oil–in-water (w/o/w) double emulsion solvent evaporation method. Briefly, 8 mg of PLGA 50:50 (MW = 15 kDa) was dissolved in 0.75 ml of dichloromethane–ethyl acetate (DCM–EA) (1/1, v/v) as organic phase. The organic phase was emulsified with the mixture of 125 μl of calcium precursor solution and 125 μl of phosphate precursor solution by probe sonication at certain amplitude for 50 s in ice bath (Tekmar Sonic Disruptor TM300, Mason, Ohio). The primary emulsion was added dropwise to 3 ml of 1% (w/v) PVA solution and the mixture was sonicated for 50 s followed by rotary evaporation under vacuum to remove the organic solvents at 37 °C (Rotavapor R-114, Büchi, Switzerland). The unencapsulated pDNA was separated from the nanoparticles by centrifugation at 13,300 rpm at 4 °C for 90 min (Eppendorf, Germany). The supernatant was used for determination of the unencapsulated pDNA, and the nanoparticles were resuspended in deionized water before use. Blank nanoparticles were prepared as mentioned above except for replacing pDNA with buffer TE (10 mM Tris–Cl, 1 mM EDTA, pH 8.0).

CaPi-pDNA-PLGA-MPs were made as previously established by Li et al. (2004). Briefly, 0.6 ml of CaPi-pDNA solution containing 36 μg pDNA was emulsified in 2 ml of dichloromethane (DCM) containing PLGA 50:50 (MW = 40–75 kDa) with a Ultra-Turrax Homogenizer (IKA T10 basic, IKA Werke GmbH and Co., Germany) for 5 s at 7500 rpm to form primary emulsion (W/O). Thereafter, the primary emulsion was added into 10 ml of the PVA aqueous solution (3.0%, w/v) and homogenized at 7500 rpm in an ice bath for 5 s (IKA T10 basic, IKA Werke GmbH and Co., Germany). The double emulsion (W/O/W) was diluted in 20 ml PVA solution (0.5%, w/v) under moderate magnetic stirring at ambient temperature for 2 h to allow solidification of the microparticles and evaporation of the solvent.

pDNA-PLGA-NPs were prepared using the same method as CaPi-pDNA-PLGA-NPs except the inner aqueous phase of primary emulsion was made up of pDNA water solution.

CaPi-pDNA co-precipitation was prepared by a slight modification of a method described by Yang and Yang (1997). pDNA solution was mixed with 2.5 M $CaCl_2$. This solution was slowly added to 1 ml of 2× HBS (containing 0.28 M NaCl, 10 mM KCl, 1.5 mM $Na_2HPO_4{\cdot}2H_2O$, 50 mM dextrose, 40 mM HEPES) at pH 7.0 under gentle vortexing. This mixture was allowed to stand for 20 min before use. At the end of titration, sterilized, deionized water was added to give a final volume. The samples were lyophilized when analyzed in Sections 2.4–2.6.

In this study, the effect of various parameters on the mean diameter, pDNA encapsulation efficiency, plasmid integrity and bioactivity in vitro were assessed. The parameters included MW and HD of PVA, Ca/P ratio, initial concentration of $CaCl_2$, the composition of organic phase, sonication time and sonication energy and aqueous phase pH. Apart from stated exceptions, all the experiments were conducted by changing one of the parameters while keeping all the other parameters at a set of standard conditions: 1% (w/v) PLGA in 0.75 ml of DCM:ethyl acetate (EA) mixture (1:1, v/v) as the organic phase, and 3 ml of 1% PVA (MW: 30,000–70,000, HD: 87–90%) solution as the aqueous phase. The initial concentration of $CaCl_2$ was 2.5 M and the Ca/P ratio was 250. The time of sonication was 50 s plus 50 s at 39.6 W. The organic solvent was rapidly removed under vacuum at 37 °C.

All batches of the particles were produced at least in triplicate.

2.2.2. Encapsulation efficiency

The encapsulation efficiency was calculated by dividing the pDNA amount in the particle fraction by the amount of pDNA added initially. The amount of pDNA in the particle fraction was indirectly calculated by subtracting the amount of unencapsulated pDNA in the supernatant from the amount of pDNA added initially. The amount of pDNA was quantified by DNA fluorometric assay using Hoechst dye 33258 as described in previous study (Rago et al., 1990). 200 μl of the supernatant (see Section 2.3) was then mixed with 3.8 ml Hoechst 33258 solution (0.15 μg/ml). The fluorescence intensity was determined on a fluorescence spectrophotometer at an excitation wavelength of 356 nm and an emission wavelength of 465 nm (LS35, Perkin-Elmer, Norwalk, CT). The amount of pDNA was calculated using a standard curve method.

2.2.3. Particle size and zeta potential

The nanoparticle size distribution and ζ potential were measured by dynamic light scattering on a Zetasizer ZEN3600 particle sizer (Malvern Nano-ZS 90 laser particle size analyzer, UK). The average nanoparticle size was expressed as the volume mean diameter n_{md} (nm).

2.2.4. Agarose gel electrophoresis

The particles were prepared as described in Section 2.3. Dichloromethane was used to dissolve the nanoparticles. After dissolution, TE buffer with 1% (w/v) heparin sodium was added to replace pDNA. 10% (v/v) loading buffer was added to the mixture and the mixture were applied to a 0.8% agarose in TBE buffer (89 mM Tris, 89 mM Boric Acid, and 2 mM EDTA, pH 8.4) containing 0.6 μg/ml ethidium bromide. Electrophoresis (Sunrise 96, Labrepco, USA) was carried out at a constant voltage of 90 V for 40 min. pDNA fragments were stained with ethidium bromide. Images under fluorescent light were captured by a gel documentation system (Bio-Rad Laboratories, Inc., Hercules, CA).

2.2.5. Transfection in vitro

HEK 293 cells were maintained in DMEM media supplemented with 10% fetal bovine serum, and 1% penicillin/streptomycin. Cells were seeded in a 6-well plate at a concentration of 10^5 cells/well one day before transfection. After 24 h, the old media were removed and replaced by fresh medium with the nanoparticles (2.7 mg pDNA per well). After 48 h of incubation with the nanoparticles, the old media were replaced with the fresh media. After another 24 h, cells were washed with PBS and imaged using an Olympus IX-70-fluorescence microscope with a dichroic filter set (EX: 475 nm, EM: 506 nm). Images were captured using NIH image software and print film. As controls, pDNA loaded nanoparticles without calcium phosphate, CaPi-pDNA complexes and CaPi-pDNA-PLGA-MPs were prepared. To measure GFP pDNA transfection efficiency, the cells were harvested and analyzed by a FACSCalibur flow cytometer (flow cytometry (FACS Canto II, BD Biosciences, San Jose, CA). Three independent experiments were conducted.

2.2.6. Release of pDNA in vitro

Approximately 8 mg of the particles (micron and submicron) were suspended in 1 ml of Tris–EDTA buffer (pH 7.4) containing 0.02% sodium azide as release medium at 37 °C on a horizontal shaker at 100 rpm. Samples were taken at 30 min and 12 h, 1, 2, 3, 4, 5, 6, 7 days, and once a week in the following four weeks. At each time point, the particle suspensions were ultracentrifuged at 13,300 rpm, and the supernatant was completely withdrawn. The concentrations of the pDNA released in the supernatant were determined by Hoechst 33258 staining assay as described in Section 2.2.2. After that, 1 ml of the fresh release medium was added to resuspend the particles.

2.3. TEM

Nanoparticles (pDNA-PLGA-NPs and CaPi-pDNA-PLGA-NPs) were analyzed on negative stain electron microscopy using a

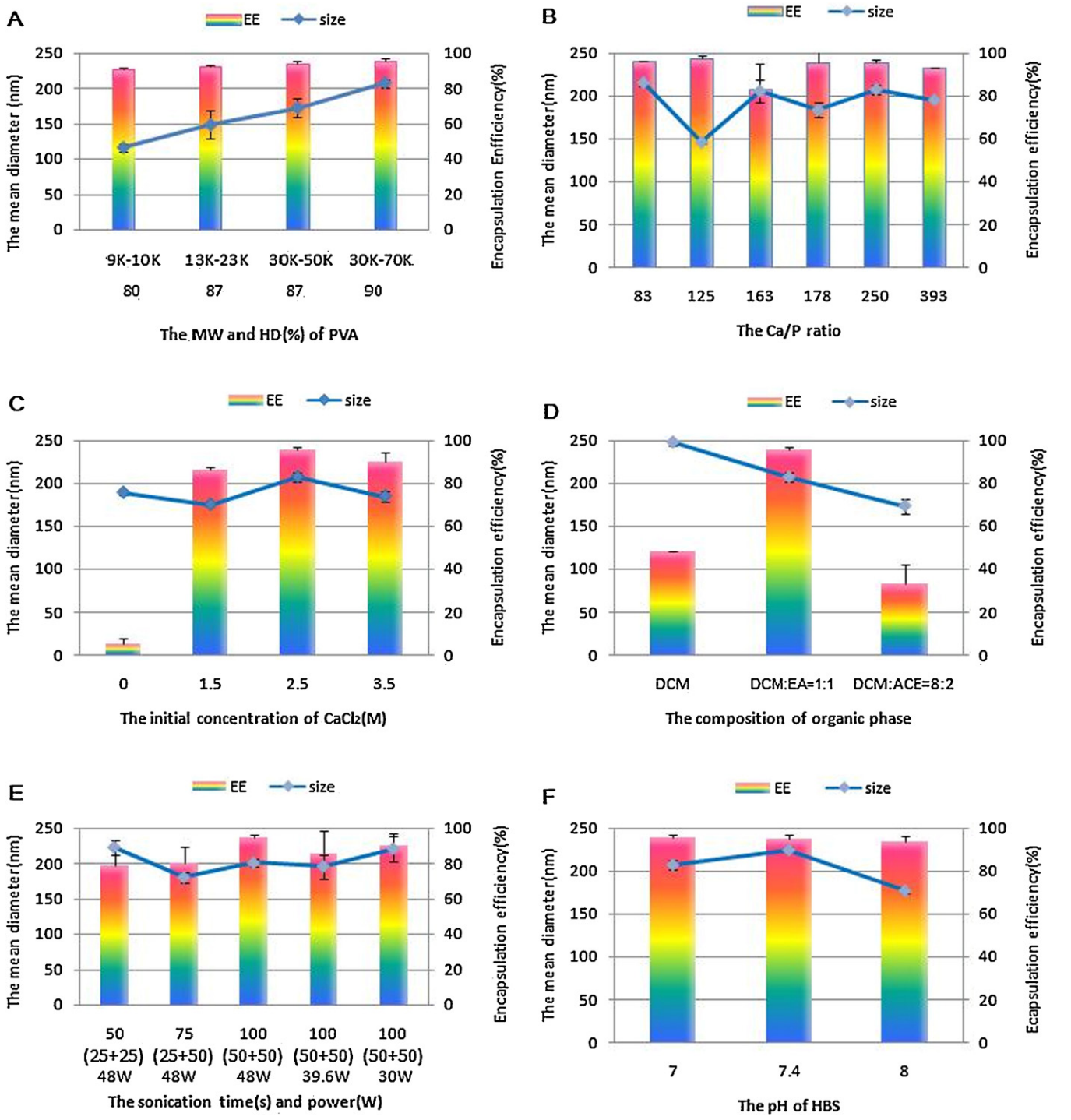

Fig. 2. Effect of various processing parameters and polymer characteristics on the mean diameter and entrapment efficiencies of the nanoparticles, including the MW and HD of PVA (A), the Ca/P ratio in the aqueous phase (B), initial $CaCl_2$ concentration (C), the composition of organic phase (D), sonication time and power (E) and aqueous phase pH (F) ($n = 3$). In (D), the abbreviations of the dichloromethane; ethyl acetate and acetone are DCM; EA and ACE; respectively.

transmission electron microscopy (H-600, Hitachi, Japan) working at 80 kV. Moreover, a Tecnai G2 F20 S-Twin TEM equipped with a scanning stage (STEM) and a high angle annular dark field (HAADF) detector was used to measure the further structural details of the nanoparticles.

2.4. DSC analysis

The thermal properties of CaPi-pDNA, blank PLGA nanoparticles, physical mixture of CaPi-pDNA powder and blank nanoparticles and CaPi-pDNA-PLGA-NPs were also analyzed by DSC (NETSCZ 204, Germany). DSC thermograms were acquired by heating lyophilized samples in sealed standard aluminum pans (TA instrument, New Castle, Delaware, USA) from 10 °C to 400 °C at a heating rate of 10 °C/min.

2.5. XRD analysis

X-ray diffractometer (X'Pert Pro, Philips, Netherlands) was utilized to study the crystalline phases of the samples. XRD studies

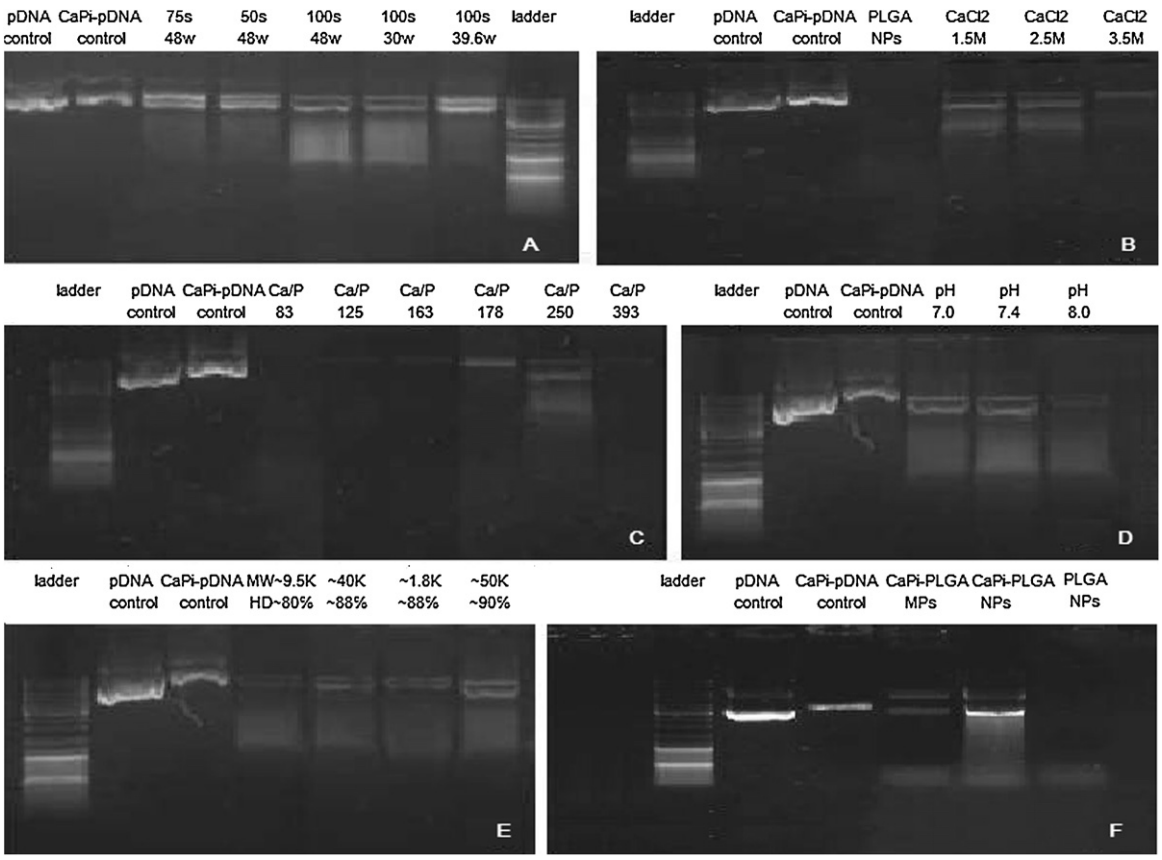

Fig. 3. Agarose gel showing the effect of ultrasonication (time and power) on plasmid DNA integrity (A); the initial concentration of $CaCl_2$ which combined with plasmid before emulsification (B); the Ca/P ratio which combined with plasmid before emulsification (C); the pH value which the Ca-Pi-DNA formed at (D) and MW and HD of PVA which used as emulsifier (E); size of delivery system (micron and submicron particles) (F) on plasmid DNA integrity.

were performed by exposing samples to CuKa radiation (40 kV, 20 mA). Lyophilized samples used for XRD analysis were CaPi-pDNA, pDNA-PLGA-NPs and CaPi-pDNA-PLGA-NPs.

2.6. Surface area and pore size determination (PSD)

The specific surface area and pore size distribution of CaPi-pDNA-PLGA-NPs and pDNA-PLGA-NPs were measured by the BET adsorption method with nitrogen gas using an accelerated surface area and porosimetry system (ASAP 2010).

3. Results and discussion

3.1. Formulation screening of CaPi-pDNA-PLGA-NPs

3.1.1. Factors affecting the mean diameter and the pDNA entrapment efficiencies of CaPi-pDNA-PLGA-NPs

In this study, the effect of 8 preparation variables on the mean diameter and the pDNA entrapment efficiency of CaPi-DNA-NPs were investigated. The results are demonstrated in Fig. 2.

Fig. 2A shows that the diameter of the nanoparticles increased with the increase of the MW of PVA ($p < 0.05$). This was contributed to the decrease of the net shear stress caused by the increase of the viscosity of internal phase, which promoted the formation of droplets with large size (Song et al., 2008). And both the MW and HD of PVA had no significant influence on pDNA entrapment efficiency ($p > 0.05$).

In Fig. 2B, the Ca/P ratio had no significant influence on the diameter of the nanoparticles ($p > 0.05$). However, when Ca/P ratio was at 83,125,163, visible calcium phosphate precipitates were generated during the process of making primary emulsion, and they failed to be encapsulated into aqueous phase of the primary emulsion. Though the pDNA encapsulation efficiency was high, the CaPi embedded PLGA nanoparticles were not formed.

In Fig. 2C, it is important to note that the pDNA was not efficiently incorporated into the PLGA nanoparticles without $CaCl_2$ in the formulation. When the initial concentration of $CaCl_2$ increased from 1.5 M to 2.5 M, the entrapment efficiency of pDNA increased ($p < 0.05$). It was probably because that the pre-condensation of pDNA with optimal calcium phosphate reduced pDNA loss during fabrication (Blum and Saltzman, 2008). However, the initial $CaCl_2$ concentration had no significant influence on the particle size of the nanoparticles ($p > 0.05$).

The mean diameter of the nanoparticles was significantly influenced by the composition of organic phase ($p < 0.05$) as demonstrated in Fig. 2D. The nanoparticles made with the organic phase containing acetone had the smallest particle size. The rapid dispersion of acetone (ACE) into the external aqueous phase contributed to a conspicuous reduction of the interfacial tension, thereby decreasing the particle size. Since ethyl acetate (EA) was partially water-miscible, the formulation containing it gave a medium particle size. These results were consistent with previous literature (Niwa et al., 1993, 1994). Meanwhile, it was interesting to find that the formulation using DCM–EA mixture (1:1, v/v) as the organic phase had higher encapsulation efficiency than those using either DCM or DCM–ACE (Fig. 1D). A common idea that fast polymer precipitation can prevent drug dispersion into the continuous phase was the basis of most attempts to increase encapsulation efficiency (Bodmeier and McGinity, 1988). The rapid solidification of PLGA matrices caused by EA in the oil phase contributed to the high pDNA entrapment efficiency (always above 80%) (Yeo and Park, 2004; Tinsley-Bown et al., 2000). Fig. 2E shows that the mean diameter

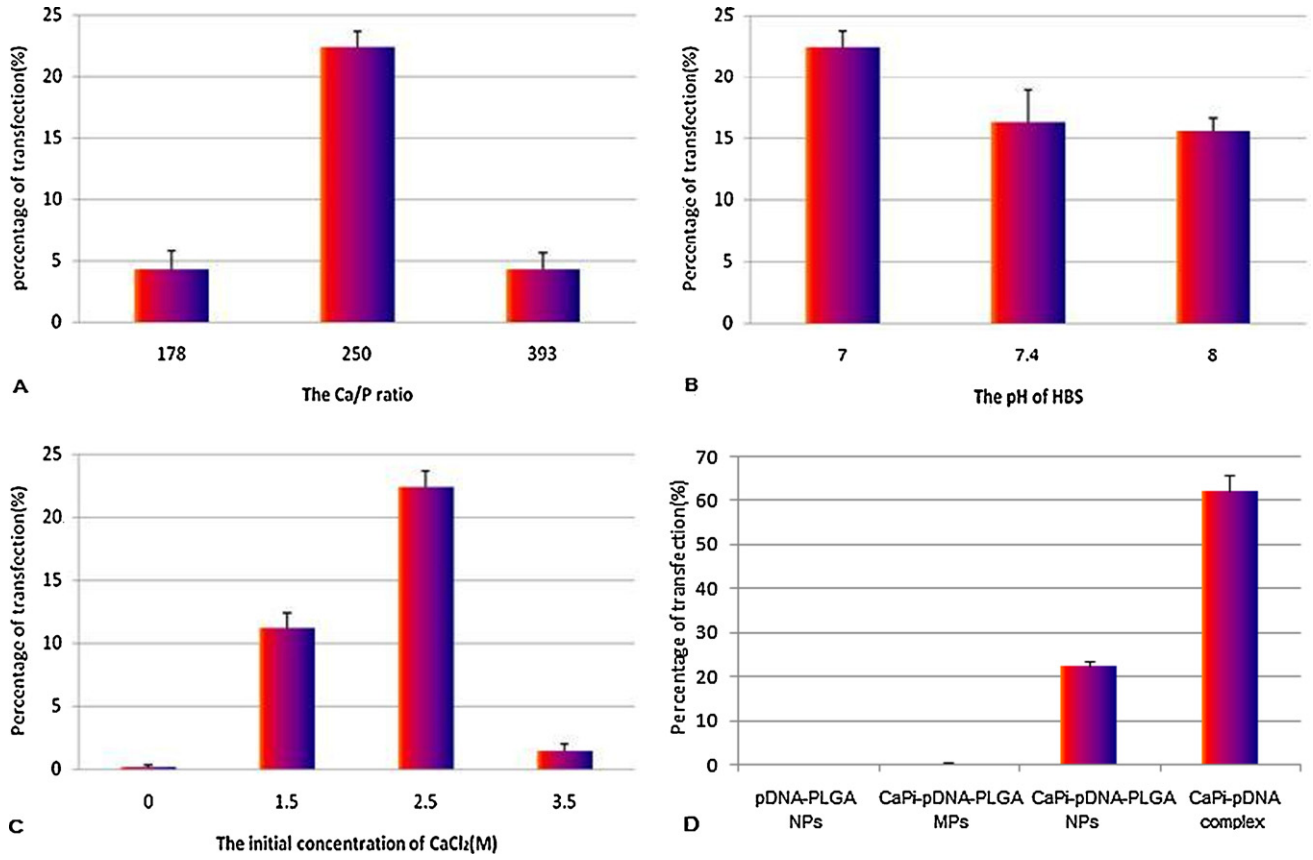

Fig. 4. Effect of several parameters on transfection efficiency of CaPi-pDNA-PLGA-NPs including the Ca/P ratio (A), the pH of HBS (B) and the initial concentration of $CaCl_2$ (C). The transfection efficiency of pDNA-PLGA-NPs, CaPi-pDNA-PLGA-MPs, optimized CaPi-pDNA-PLGA-NPs and CaPi-pDNA complexes. All results were detected by FCM.

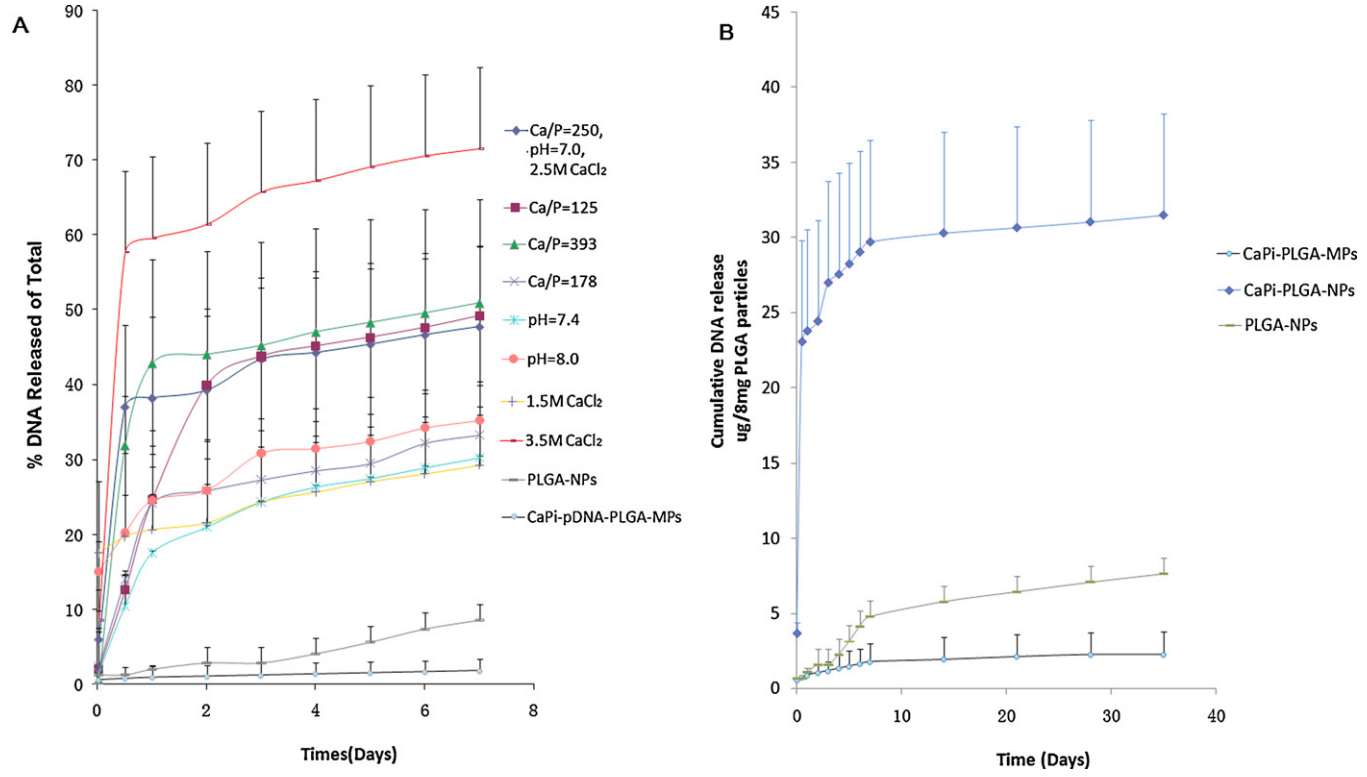

Fig. 5. The cumulative release of pDNA from the particles. (A) In the first 7 days. The basic formulation was described in Section 2.2.1 (pH 7.0, 2.5 M $CaCl_2$, Ca/P = 250) (♦). The changed parameter in other formulations has been listed by the side of the symbols. Errors bars indicate standard deviation ($n = 3$). (B) The cumulative pDNA (ng) release of CaPi-pDNA-PLGA-NPs (♦) (pH7.0, 2.5 M $CaCl_2$, Ca/P = 250), CaPi-pDNA-PLGA-MPs (●) and pDNA-PLGA-NPs (–) from 1 to 5 weeks.

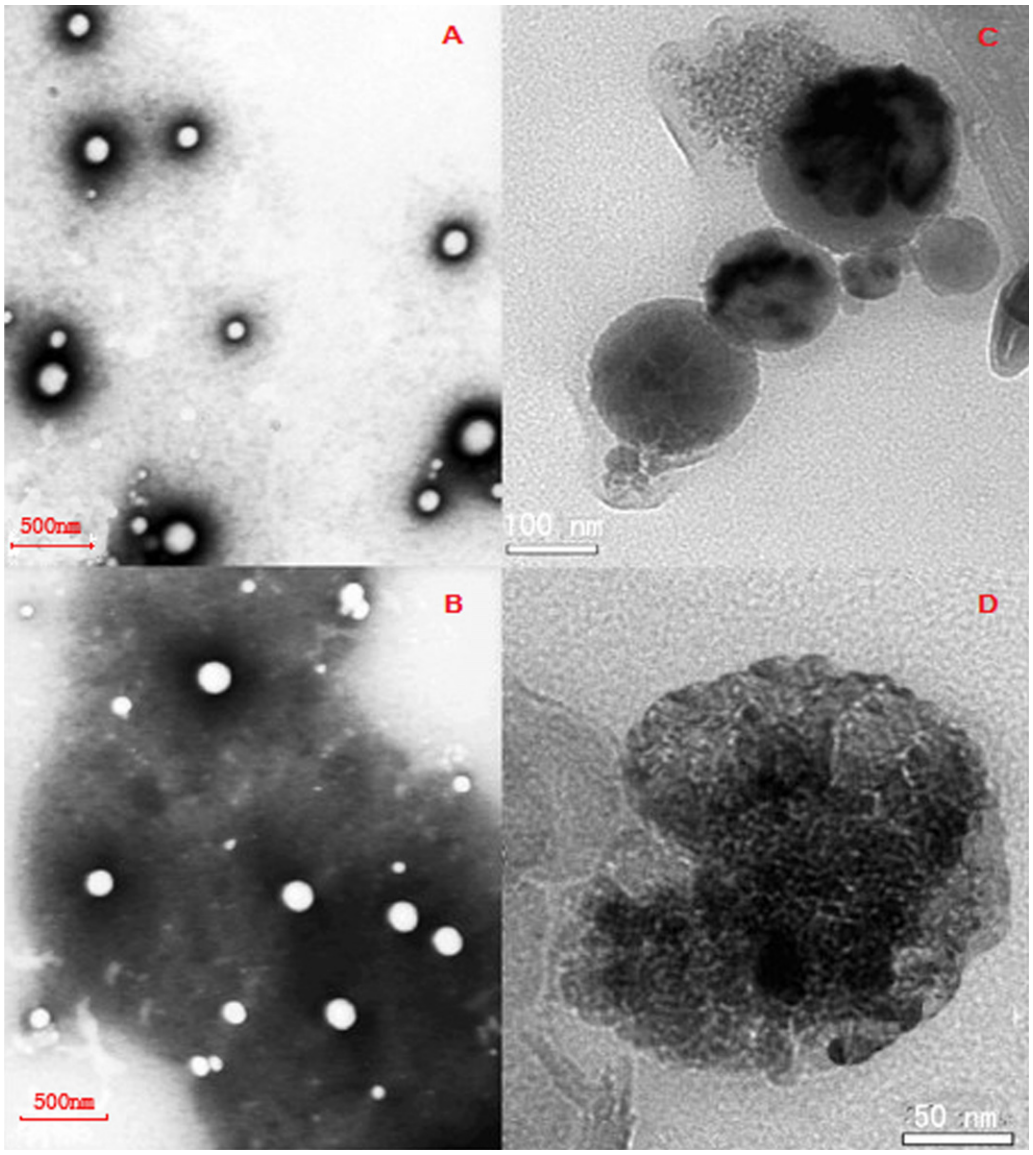

Fig. 6. TEM images of pDNA-PLGA-NPs (A and C) and CaPi-pDNA-PLGA-NPs (B and D). (A) and (B) were of low magnification; (C) and (D) were of high magnification.

first decreased and then reached a plateau when the sonication time increased, which was similar to the results reported in literature (Kwon et al., 2001; Mainardes and Evangelista, 2005). Three kinds of sonication time (including 50 s, 75 s and 100 s) were adopted for the preparation of the nanoparticles. For 50 s, 25 s and 25 s were used for making the primary emulsion and the secondary emulsion, respectively. For 75 s, 25 s and 50 s were used for making the primary emulsion and the secondary emulsion, respectively. For 100 s, 50 s and 50 s were used for making the primary emulsion and the second emulsion, respectively. The mean diameter of the nanoparticles was reduced simply by increasing the sonication time in the secondary emulsification process ($p < 0.05$), while it was not influenced by the extension of sonication time in the primary emulsification process. The result suggested that the sonication time in the secondary emulsification process had greater influence on the mean diameter, which was consistent with previous research (Bilati et al., 2003). Meanwhile, high sonication power did not result in further decrease of the mean diameter indicating that it was sufficient to induce rapid formation of spherical-shaped droplets of submicronic size at 39.6 W (Fig. 2E). No significant disparity occurred in the pDNA entrapment efficiency among the formulations with different sonication time and energy. This result suggests that the lowest sonication energy (30 W) and the shortest sonication time (50 s) used in this study were enough to fabricate the nanoparticles.

As shown in Fig. 2F, there is no significant difference in diameter between formulations prepared at pH 7.0 and pH 7.4, while the diameter of the formulation prepared at pH 8.0 decreased ($p < 0.05$). This was probably ascribed to the increased size of the CaPi-pDNA complexes when the aqueous phase pH increased (Li et al., 2004). As the complexes prepared at pH 8.0 were too large to be encapsulated into the PLGA nanoparticles, the small diameter of the nanoparticles at pH 8.0 suggested the leakage of the CaPi-pDNA complexes. And according to Fig. 1F, pH value of aqueous phase had no significant influence on pDNA entrapment efficiency ($p > 0.05$).

In addition, it was found that the encapsulation efficiencies of the 20 different formulations of CaPi-pDNA-PLGA-NPs were all high than that of CaPi-pDNA-PLGA-MPs ($46.9 \pm 2.5\%$ prepared using DCM and $77.9 \pm 0.5\%$ prepared using DCM–EA mixture (1:1, v/v) with a mean diameter of 1.3 ± 0.2 μm. This indicated that the CaPi embedded submicron system was more advantageous in encapsulating pDNA than the micron system, which may result from relative large surface area of the former as discussed in Section 3.4.

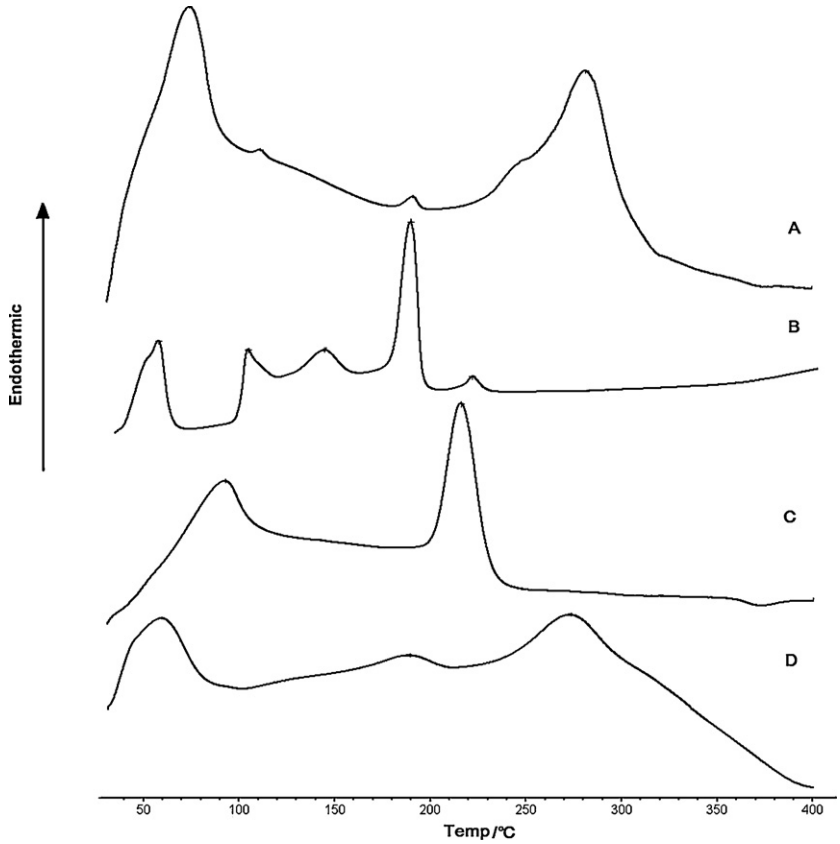

Fig. 7. The DSC curves of (A) physical mixture of CaPi-pDNA and blank PLGA-NPs, (B) CaPi-pDNA, (C) CaPi-pDNA-PLGA-NPs, and (D) pDNA-PLGA-NPs.

3.1.2. Factors affecting integrity of the encapsulated pDNA

The structural integrity of the pDNA has been reported to affect its transfection efficiency in cells (Tinsley-Bown et al., 2000). Some research suggests that linear pDNA is much less efficient in transfection than supercoiled pDNA (Kimoto and Taketo, 1996; Xie et al., 1992). Thus, the structural integrity of the encapsulated pDNA needs to be considered when screening the formulations.

Additionally, shear stress given by sonication has been demonstrated to affect the integrity of pDNA during encapsulation processes (Walter et al., 2001). Extensive shear stress results in DNA fragmentation (Levy et al., 1999). In Fig. 3A, it is showed that the original pDNA before encapsulation was predominantly supercoiled with a small amount of linear pDNA. The five recovered samples showed less supercoiled pDNA and correspondingly more linear pDNA with a ratio around 1:1. The formulation with a sonication power of 39.6 W and a sonication time of 100 s gave the brightest band as it gave the best protection for pDNA and was adopted.

Fig. 3B shows that the condensation of pDNA by calcium phosphate increased the stability of pDNA. It is well known that calcium and other polyvalent metal cations can form ionic complexes with the phosphate groups of DNA and compact the DNA molecules (Bloomfield, 1997). The protection of pDNA from destruction by shearing force in sonication process was due to the close-knit, well organized structure of the complexes. The increased concentration of $CaCl_2$ did not significantly contribute to the stability of the pDNA. However, high concentration of $CaCl_2$ (3.5 M) lost the condensing capacity of pDNA, and had poor protection of pDNA, which is consistent with previous research (Pedraza et al., 2008). So, $CaCl_2$ with a concentration of 1.5 M was enough to condense pDNA.

The protection of pDNA by calcium phosphate at various Ca/P ratios was shown in Fig. 3C. When Ca/P ratio was at 83,125,163, visible calcium phosphate precipitates were generated before the primary emulsion was formed. The replacement of pDNA by heparin from the precipitates was incomplete. When the Ca/P ratio was higher than 250, calcium phosphate was not able to condense plasmid efficaciously, leading to a degradation of pDNA during sonication process. Consequently, the electrophoresis strip of supercoiled pDNA vanished. Considerable amount of supercoiled pDNA remained only when the Ca/P ratio was at 250 (Fig. 3B). At this ratio, pDNA was completely condensed and no visible precipitate was formed. Therefore, the pDNA was well protected from the shear stress during sonication.

The influence of pH on the stability of CaPi-pDNA is shown in Fig. 3D. As shown in Fig. 3C, CaPi-pDNA prepared at pH 7.0 and 7.4 showed good stability. When pH 8.0, the CaPi-pDNA complexes formed precipitates and were not encapsulated into the PLGA nanoparticles. So, the pDNA was easily damaged, which was consistent with previous study (Li et al., 2004).

The protection of CaPi-pDNA by PVA is shown in Fig. 3E. PVA with high HD contained a large number of hydroxyl groups which was able to form hydrogen bonds between intra- or intermolecules, which would result in the increase of the aqueous phase viscosity and, consequently, the reduction of the net shear stress to pDNA (Hong et al., 2001; Lewandowska et al., 2001; Li et al., 2000; Lyoo et al., 2003). Meanwhile, the increasing MW of PVA also led to increase in viscosity of continuous phase, which also decreased the net shear stress. Hence, pDNA denaturation was prevented by using PVA with high MW and HD.

The pDNA integrity of the micron and the submicron particles is shown in Fig. 3F. Ultrasonic emulsification was used when preparing CaPi-pDNA-PLGA-NPs, and Ultra-Turrax treatment was used for preparing CaPi-pDNA-PLGA-MPs. Emulsification method was the most important difference between their preparation processes, which accounted for their difference in pDNA integrity. The result is consistent with previous work (Kofler et al., 1996; Ian et al., 2002),

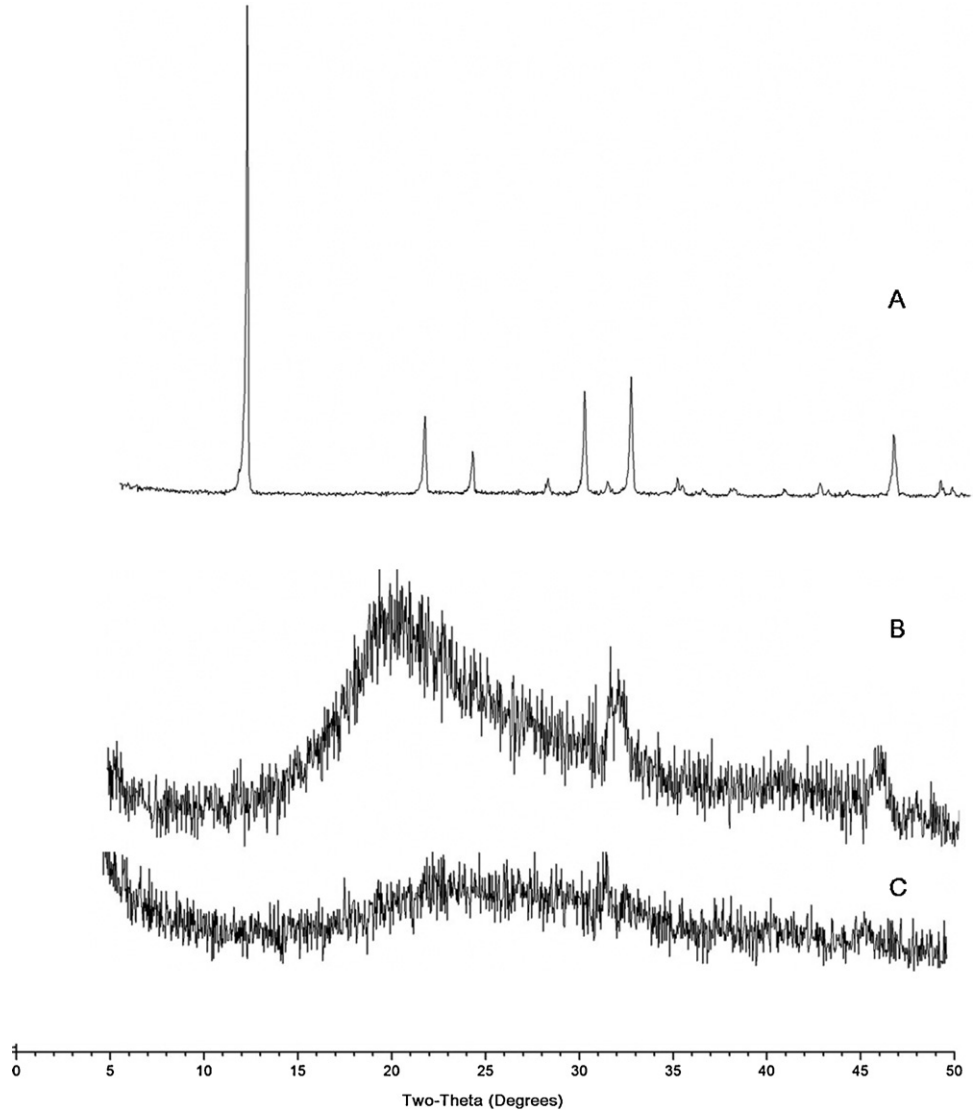

Fig. 8. XRD patterns of (A) CaPi-pDNA, (B) pDNA-PLGA-NPs, and (C) CaPi-pDNA-PLGA-NPs.

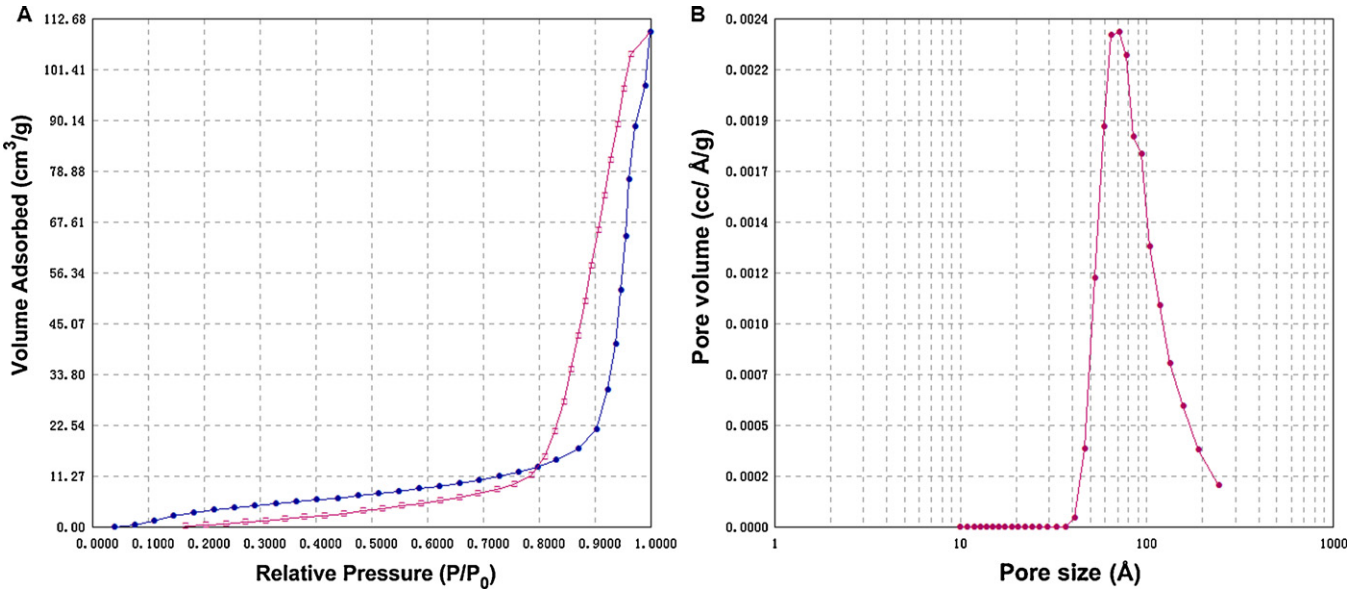

Fig. 9. N_2 adsorption–desorption isotherm (A) and the corresponding BJH pore size distribution curve (B) of CaPi-pDNA-PLGA-NPs.

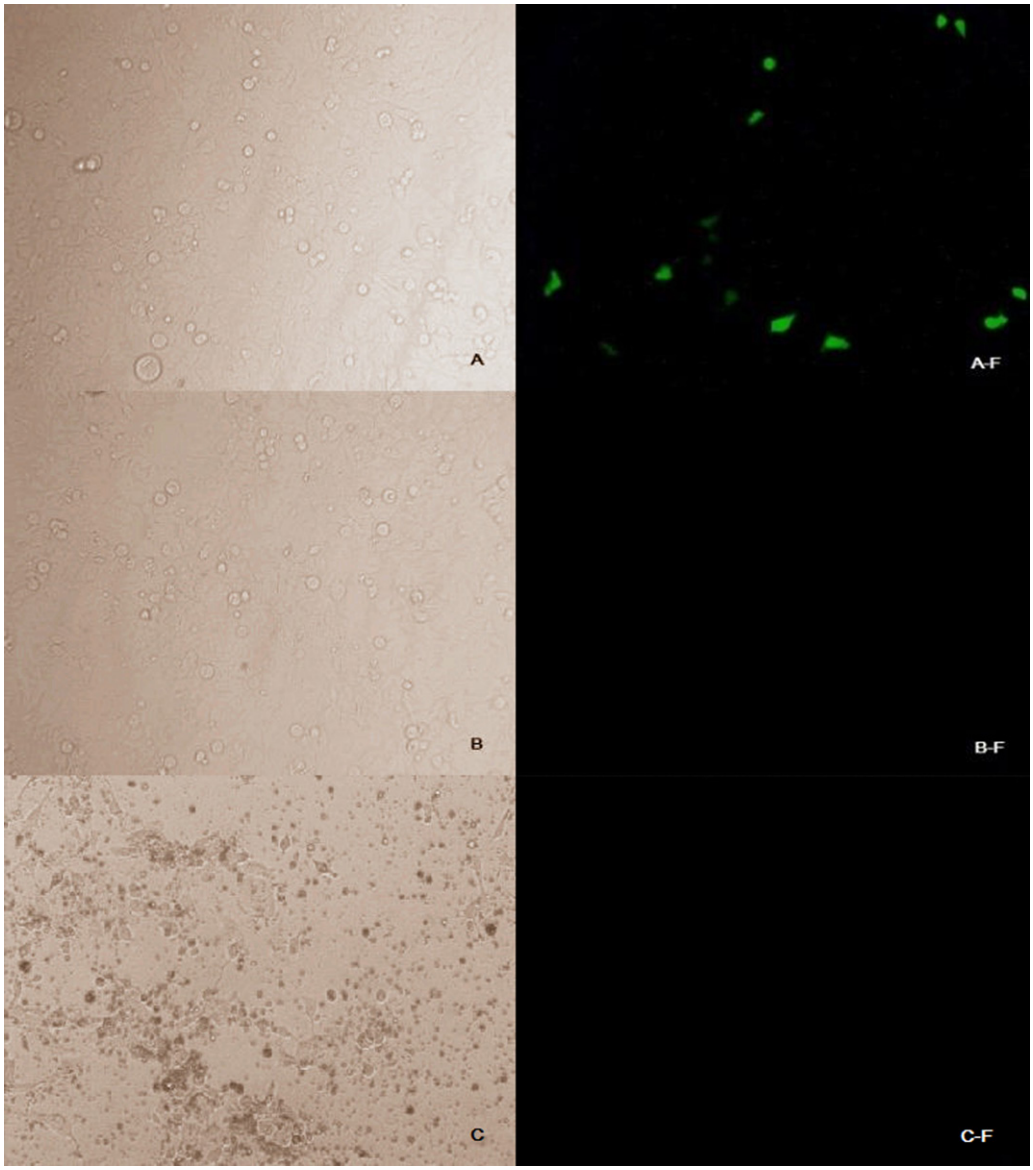

Fig. 10. Transmission light microscope pictures (the first panel) and GFP fluorescence microscope pictures (the second panel) of 293 cells transfected with CaPi-pDNA-PLGA-NPs after optimization (A), pDNA-PLGA-NPs (B) and CaPi-pDNA-PLGA-MPs (C).

which has showed that Ultra-Turrax treatment would affect the stability of macromolecules incorporated within the particles much more than ultrasonic.

3.1.3. Transfection in vitro

The effect of three preparing parameters, including Ca/P ratio, pH, $CaCl_2$ concentration, on the transfection efficiency of different vehicles were studied (Fig. 4). Formulation with a Ca/P ratio of 250 gave a higher transfection efficiency than the formulations with Ca/P ratio of 178 or 393, which was due to the better protection of pDNA according to the electrophoresis described above (Fig. 4A). The formulation made at pH 7 achieved better transfection relative to formulations made at both pH 7.4 and pH 8, which was ascribed to the good stability of the complexes formed at pH 7 (Fig. 4B). The formulations with $CaCl_2$ concentration of both 1.5 M and 2.5 M gave higher transfection efficiency than the formulation with a $CaCl_2$ concentration of both 3. 5 M because of the very compact CaPi-pDNA complexes formed under these concentrations, which protected pDNA from shearing force as discussed in Section 3.1.2 (Fig. 4C). pDNA-PLGA-NPs and CaPi-pDNA-PLGA-MPs almost had no gene transfection probably due to the low encapsulation efficiency and the slow release rate of pDNA. CaPi-pDNA co-precipitates achieved very high transfection efficiency around $60 \pm 3.5\%$ (Fig. 4D). As we all know, calcium phosphate was a traditional transfection agent, however, its use was limited by its poor stability and reproducibility (Sokolova et al., 2006).

3.1.4. Release of pDNA from nanoparticles in vitro

The influence of several factors, including the initial concentration of $CaCl_2$, Ca/P ratio and pH of inner aqueous phase, etc., on the pDNA release in vitro from CaPi-pDNA-PLGA-NPs was investigated. Besides, release of pDNA from CaPi-pDNA-PLGA-MPs was also studied (Fig. 5).

By comparing the release of formulation with different $CaCl_2$ concentrations, it was found out that increasing $CaCl_2$ concentration prompted burst release of the pDNA (Fig. 5A). This might be caused by the faster fluid exchange between inside and outside of the nanoparticles driven by a osmotic pressure gradient under high salt concentration. Formulation prepared at pH 7.0 had higher release rate relative to formulations prepared at pH 7.4 and pH 8,

respectively. With the increase of ratio of Ca/P, the burst release increased on the first day. It was probably because the ability of the CaPi to condense pDNA decreased with the increase of Ca/P ratio. CaPi-pDNA-PLGA-MPs exhibited a much slower release rate relative to CaPi-pDNA-PLGA-NPs and pDNA-PLGA-NPs. The release of pDNA from CaPi-pDNA-PLGA-MPs was hindered by thick spherical shell and the slow erosion of the polymer. The pDNA release of pDNA-PLGA-NPs was higher than that of CaPi-pDNA-PLGA-MPs probably due to the larger surface area.

3.1.5. Optimization of CaPi-pDNA-PLGA-NPs

To verify the optimal parameters, CaPi-pDNA-PLGA-NPs were subsequently prepared as follows: 8 mg PLGA was dissolved in 0.75 ml of dichloromethane-ethyl acetate (1/1, v/v) as organic phase. The organic phase was emulsified with the mixture of 125 μl of calcium precursor solution containing pDNA (2.5 M) and 125 μl of phosphate precursor solution (pH 7.0) at a Ca/P ratio of 250 by probe sonication at 39.6 W for 50 s in ice bath. The primary emulsion was added to 1% (w/v) PVA (MW: 30,000–70,000, HD: 87–90%) solution and the mixture was sonicated for 50 s followed by rapid evaporation under reduced pressure to remove the solvent. The unencapsulated pDNA was separated from the nanoparticles by centrifugation at 13,300 rpm at 4 °C for 90 min.

3.2. Morphology of nanoparticles

Morphology of the NPs was examined under both high magnification and low magnification TEM (Fig. 6). Under low magnification, it was observed that pDNA-PLGA-NPs and CaPi-pDNA-PLGA-NPs were spherical in shape (Fig. 6A and B). However, the high magnification images indicated the pDNA-PLGA-NPs were spheres with smooth surface, while the CaPi-pDNA-NPs had uneven surface (Fig. 6C and D).

3.3. DSC and XRD analysis

The DSC thermograms of several samples are shown in Fig. 7. pDNA-PLGA NPs have endothermic peaks at 58.6 °C and 272.6 °C, respectively. CaPi-pDNA has an endothermic peak at 190.2 °C. All of these characteristic peaks were observed in the thermogram of physical mixture of the CaPi-pDNA and the pDNA-PLGA-NPs. As the amount of CaPi-pDNA in the mixture was low, its characteristic peak was small. In the thermogram of CaPi-pDNA-PLGA-NPs, the peak of CaPi-pDNA disappeared and the peak of PLGA-NPs at 58.6 °C shifted right and a new peak at 219.6 °C arised, which proved the interaction between the CaPi-pDNA and the PLGA. XRD was performed to identify crystalline phase of the CaPi-pDNA-PLGA-NPs and the results are presented in Fig. 8. In XRD pattern of CaPi-pDNA, it exhibited a sharp peak at about 2θ scattered angle 12 indicating crystalline nature of CaPi-pDNA. This characteristic peak for CaPi-pDNA was absent in the XRD pattern of CaPi-pDNA-PLGA-NPs, suggesting that CaPi-pDNA was in weak crystallization form in the nanoparticles.

3.4. Surface area and pore size distribution (PSD)

Fig. 9 exhibits the N_2 adsorption–desorption isotherm (A) and the corresponding Banett–Joyner–Halenda (BJH) pore size distribution curve of the CaPi-pDNA-PLGA-NPs (B). According to the IUPAC definition, the isotherm of CaPi-pDNA-PLGA-NPs was attributed to type IV, which was porous structure. The measurement shows that the BET specific surface area of the CaPi-pDNA-PLGA-NPs was 57.5 m^2/g and the BJH desorption average pore size was about 96.5 Å. The large surface area and porous structure are advantageous for pDNA release. Upon exposure to the release medium, the CaPi-pDNA complexes on the surface of the nanoparticles dissolved quickly. And a considerable number of porous channels may form resulting in a fast release of the pDNA described in Section 3.1.4. Our results are in accordance with the model proposed by Lemaire et al. (2003), where authors suggested that the effective diffusion coefficient of the drug molecule in the wetted polymer, the average pore length and the initial pore diameter are the most critical parameters determining the release behavior, whereas other parameters related to total and external surface area played minor roles.

3.5. Transfection image

Transfection images of different samples are shown in Fig. 10. It was found that GFP expression of CaPi-pDNA-PLGA-NPs was significantly higher than that of pDNA-PLGA-NPs and CaPi-pDNA-PLGA-MPs, which is consistent with the result in Section 3.1.3.

4. Conclusion

The effect of several preparation factors on the particle size, incorporation efficiency, release behavior in vitro and transfection efficiency was studied by Single Factor Screening Method. These preparation factors included the MW, HD of PVA, sonication power, sonication time, composition of organic phase, initial concentration of calcium phosphate and Ca/P ratio, etc. CaPi-pDNA-PLGA-NPs produced by the optimal formulation exhibited spherical shape with a particle size of 207 ± 5 nm, zeta potential of -2.18 ± 0.17 mV. Its transfection efficiency was remarkably increased relative to pDNA-PLGA-NPs. The XRD and DSC studies indicated that CaPi-pDNA was in weak crystallization form inside the nanoparticles. BET measurements demonstrated that CaPi-pDNA-PLGA-NPs had mesoporous structure with an average pore size of 96.5 Å and a relative large specific surface area. Further studies are needed to illustrate practical benefit of these particles in vivo.

Acknowledgments

This work was supported by National Natural Science Foundation of China (81001012).

Conflict of interest: The authors report no conflicts of interest. The authors alone are responsible for the content and writing of this paper.

References

Aral, C., Akbuga, J., 2003. Preparation and in vitro transfection efficiency of chitosan microspheres containing plasmid DNA:poly(L-lysine) complexes. J. Pharm. Pharm. Sci. 6, 321–326.

Bilati, U., Allémann, E., Doelker, E., 2003. Sonication parameters for the preparation of biodegradable nanocapsules of controlled size by the double emulsion method. Pharm. Dev. Technol. 3, 1–9.

Bloomfield, V.A., 1997. DNA condensation by multivalent cations. Biopolymer 44, 269–282.

Blum, J.S., Saltzman, W.M., 2008. High loading efficiency and tunable release of plasmid DNA encapsulated in submicron particles fabricated from PLGA conjugated with poly-L-lysine. J. Control. Release 129, 66–72.

Bodmeier, R., McGinity, J.W., 1988. Polylactic acid microspheres containing quinidine base and quinidine sulphate prepared by the solvent evaporation method. III. Morphology of the microspheres during dissolution studies. J. Microencapsul. 5, 325–330.

Coelho, E.A.F., Tavares, C.A.P., Lima, K.D., Silva, C.L., Rodrigue, J.M., Fernandes, A.P., 2006. Mycobacterium hsp65 DNA entrapped into TDM-loaded PLGA microspheres induces protection in mice against Leishmania (Leishmania) major infection. Parasitol. Res. 98, 568–575.

Denis-Mize, K.S., Dupuis, M., Singh, M., Woo, C., Ugozzoli, M., O'Hagan 3rd., D.T., Donnelly, J.J., Ott, G., McDonald, D.M., 2003. Mechanisms of increased immunogenicity for DNA-based vaccines adsorbed onto cationic microparticles. Cell. Immunol. 225, 12–22.

Gao, X., Kim, K.S., Liu, D., 2007. Nonviral gene delivery: what we know and what is next. AAPS J. 9, E92–E104.

He, X., Jiang, L., Wang, F., Xiao, Z., Li, J., Liu, L.S., Li, D., Ren, D., Jin, X., Li, K., He, Y., Shi, K., Guo, Y., Zhang, Y., Sun, S., 2005a. Augmented humoral and cellular immune

responses to hepatitis B DNA vaccine adsorbed onto cationic microparticles. J. Control. Release 107, 357–372.
He, X.W., Wang, F., Jiang, L., Li, J., Liu, S.K., Xiao, Z.Y., Jin, X.Q., Zhang, Y.N., He, Y., Li, K., Guo, Y.J., Sun, S.H., 2005b. Induction of mucosal and systemic immune response by single-dose oral immunization with biodegradable microparticles containing DNA encoding HBsAg. J. Gen. Virol. 86, 601–610.
Hedley, M.L., 2003. Formulations containing poly(lactide-co-glycolide) and plasmid DNA expression vectors. Expert Opin. Biol. Ther. 3, 903–910.
Hong, P.D., Chou, C.M., He, C.H., 2001. Solvent effects on aggregation behavior of polyvinyl alcohol solutions. Polymer 42, 6105–6112.
Ian, R., Steven, B., Nicholas, E.H., Richard, A.P., 2002. Influence of processing method on the exfoliation process for organically modified clay systems. I. polyurethanes. J. Appl. Polym. Sci. 91, 1335–1343.
Kimoto, H., Taketo, A., 1996. Studies on electrotransfer of DNA into *Escherichia coli*: effect of molecular form of DNA. Biochim. Biophys. Acta 1307, 325–330.
Kwon, H.-Y., Lee, J.-Y., Choi, S.-W., Jang, Y., Kim, J.-H., 2001. Preparation of PLGA nanoparticles containing estrogen by emulsification–diffusion method. Colloids Surf. A 182, 123–130.
Labhasetwar, V., Bonadio, J., Goldstein, S., Levy, R.J., 1999. Gene transfection using biodegradable nanospheres: results in tissue culture and a rat osteotomy model. Colloids Surf. B: Biointerfaces 16, 281–290.
Ledley, F.D., 1996. Pharmaceutical approach to somatic gene therapy. Pharm. Res. 13, 1595–1614.
Levy, M.S., Sorrels, C.W., Wagner, C.W., Jackson, R.J., Barnes, R.W., Smith, S.D., 1999. Evolution of the modified Rossetti fundoplication in children: surgical technique and results. Ann. Surg. 229, 774–779.
Lewandowska, K., Staszewska, D.U., Bohdanecky, M., 2001. The Huggins viscosity coefficient of aqueous solution of poly(vinyl alcohol). Eur. Polym. J. 37, 25–32.
Li, H., Zhang, W., Xu, W., Zhang, X., 2000. Hydrogen bonding governs the elastic properties of poly(vinyl alcohol) in water, single molecule force spectroscopic studies of PVA by AFM. Macromolecules 33, 465–469.
Li, Y., Ogris, M., Pelisek, J., Röedl, M.W., 2004. Stability and release characteristics of poly(D,L-lactide-co-glycolide) encapsulated CaPi-DNA coprecipitation. Int. J. Pharm. 269, 61–70.
Lima, K.M., Santos, S.A., Lima, V.M.F., Coelho-Castelo, A.A.M., Rodrigues, J.M., Silva, C.L., 2003. Single dose of a vaccine based on DNA encoding mycobacterial hsp65 protein plus TDM-loaded PLGA microspheres protects mice against a virulent strain of Myco-bacterium tuberculosis. Gene Ther. 10, 678–685.
Loyter, A., Scangos, G., Juricek, D., Keene, D., Ruddle, F.H., 1982. Mechanisms of DNA entry into mammalian cells. II. Phagocytosis of calcium phosphate DNA co-precipitate visualized by electron microscopy. Exp. Cell Res. 139, 223–234.
Luten, J., van Nostrum, C.F., De Smedt, S.C., Hennink, W.E., 2007. Biodegradable polymers as non-viral carriers for plasmid DNA delivery. J. Control. Release 126, 97–110.
Lyoo, S.W., Seo, S.I., Ji, C.B., Kim, H.J., Kim, S.S., Ghim, D.H., Kim, C.B., Lee, J., 2003. Role of the stereosequences of poly(vinyl alcohol) in the rheological properties of syndiotacticity-rich poly-(vinyl alcohol)/water solutions. J. Appl. Polym. Sci. 88, 1858–1863.
Lemaire, V., Bélair, J., Hildgen, P., 2003. Structural modeling of drug release from biodegradable porous matrices based on a combined diffusion/erosion process. Int. J. Pharm. 258, 95–107.
Mainardes, R.M., Evangelista, R.C., 2005. PLGA nanoparticles containing praziquantel: effect of formulation variables on size distribution. Int. J. Pharm. 290, 137–144.
Navarro, J., Oudrhiri, N., Fabrega, S., Lehn, P., 1998. Gene delivery systems: bridging the gap between recombination viruses and artificial vectors. Adv. Drug Deliv. Rev. 30, 5–11.
Niwa, T., Takeuchi, H., Hino, T., Kunou, N., Kawashima, Y., 1993. Preparations of biodegradable nanospheres of water-soluble and insoluble drugs with D,L-lactide/glycolide copolymer by a novel spontaneous emulsification solvent diffusion method, and the drug release behavior. J. Control. Release 25, 89–98.
Niwa, T., Takeuchi, H., Hino, T., Kunou, N., Kawashima, Y., 1994. In vitro drug release behavior of D,L-lactide/glycolide copolymer (PLGA) nanospheres with nafarelin acetate prepared by a novel spontaneous emulsification solvent diffusion method. J. Pharm. Sci. 83, 727–732.
Ochiya, T., Nagahara, S., Sano, A., Itoh, H., Terada, M., 2001. Biomaterials for gene delivery: atelocollagen-mediated controlled release of molecular medicines. Curr. Gene Ther. 1, 31–52.
Orrantia, E., Chang, P.L., 1990. Intracellular distribution of DNA internalized through calcium phosphate precipitation. Exp. Cell Res. 190, 170–174.
Pedraza, C.E., Bassett, D.C., McKee, M.D., Nelea, V., Gbureck, U., Barralet, J.E., 2008. The importance of particle size and DNA condensation salt for calcium phosphate nanoparticle transfection. Biomaterials 29, 3384–3392.
Rago, R., Mitchen, J., Wilding, G., 1990. DNA fluorometric assay in 96-well tissue culture plates using Hoechst 33258 after cell lysis by freezing in distilled water. Anal. Biochem. 191, 31–34.
Song, X., Zhao, Y., Wu, W., Bi, Y., Cai, Z., Chen, Q., Li, Y., Hou, S., 2008. PLGA nanoparticles simultaneously loaded with vincristine sulfate and verapamil hydrochloride: systematic study of particle size and drug entrapment efficiency. Int. J. Pharm. 350, 320–329.
Sokolova, V.V., Radtke, I., Heumann, R., Epple, M., 2006. Effective transfection of cells with multi-shell calcium phosphate–DNA nanoparticles. Biomaterials 27, 3147–3153.
Tagawa, T., Manvell, M., Brown, N., Keller, M., Perouzel, E., Murray, K.D., Harbottle, R.P., Tecle, M., Booy, F., BrahimiHorn, M.C., Coutelle, C., Lemoine, N.R., Alton, E.W., Miller, A.D., 2002. Characterisation of LMD virus-like nanoparticles self-assembled from cationic liposomes, adenovirus corepeptide μ (mu) and plasmid DNA. Gene Ther. 9, 564–576.
Tinsley-Bown, A.M., Fretwell, R., Dowsett, A.B., Davis, S.L., Farrar, G.H., 2000. Formulation of poly(D,L-lactic-co-glycolic acid) microparticles for rapid plasmid DNA delivery. J. Control. Release 66, 229–241.
Van de Wetering, P., Cherng, J.Y., Talsma, H., Crommelin, D.J.A., Hennink, W.E., 1998. 2-(Dimethylamino)ethyl methacrylate based (co)polymers as gene transfer agents. J. Control. Release 53, 145–153.
Walter, E., Dreher, D., Kok, M., Thiele, L., Kiama, S.G., Gehr, P., Merkle, H.P., 2001. Hydrophilic poly(DL-lactide-co-glycolide) microspheres for the delivery of DNA to human-derived macrophages and dendritic cells. J. Control. Release 76, 149–168.
Walter, E., Moelling, K., Pavlovic, J., Merkle, H.P., 1999. Microencapsulation of DNA using poly(DL-lactide-co-glycolide): stability issues and release characteristics. J. Control. Release 61, 361–374.
Wang, D., Robinson, D.R., Kwon, G.S., Samuel, J., 1999. Encapsulation of plasmid DNA in biodegradable poly(D,L-lactic-co-glycolic acid) microspheres as a novel approach for immuno-gene delivery. J. Control. Release 57, 9–18.
Xie, T.D., Sun, L., Zhao, H.G., Fuchs, J.A., Tsong, T.Y., 1992. Study of mechanisms of electric field-induced DNA transfection. IV. Effects of DNA topology on cell uptake and transfection efficiency. Biophys. J. 63, 1026–1031.
Yeo, Y., Park, K., 2004. Control of encapsulation efficiency and initial burst in polymeric microparticle systems. Arch. Pharm. Res. 27, 1–24.
Yang, Y.W., Yang, J.C., 1997. Calcium phosphate as a gene carrier: electron microscopy. Biomaterials 18, 213–217.
Zauner, W., Farrow, N.A., Haines, A.M., 2001. In vitro uptake of polystyrene microspheres: effect of particle size, cell line and cell density. J. Control. Release 71, 39–51.
Zhu, G., Mallery, S.R., Schwendeman, S.P., 2000. Stabilization of proteins encapsulated in injectable poly (lactide-co-glycolide). Nat. Biotechnol. 18, 52–57.
Kofler, N., Ruedl, C., Klima, J., Recheis, H., Böck, G., Wick, G., Wolf, H., 1996. Preparation and characterization of poly-(D,L-lactide-co-glycolide) and poly-(L-lactic acid)microspheres with entrapped pneumotropic bacterial antigens. J. Immunol. Methods 192, 25–35.